



Free-Spinning Numerical Simulation of a Novel Vertical Axis Small Water Turbine Generator for Installation in a Water Pipeline

Werayoot Lahamornchaiyakul¹, Nat Kasayapanand^{1,*}

¹ Division of Energy Technology, School of Energy, Environment and Materials, King Mongkut's University of Technology Thonburi, 126 Pracha-Uthit Road, Bang Mod, Thungkhru, Bangkok, 10140, Thailand

ARTICLE INFO

Article history:

Received 10 December 2022

Received in revised form 11 January 2023

Accepted 10 February 2023

Available online 1 August 2023

Keywords:

In-pipe Water Turbine; Vertical-Axis Water Turbine; Computational Fluid Dynamics; Numerical Simulation

ABSTRACT

The design of a novel vertical-axis small water turbine generator for installation in a pipeline is the primary purpose of this research. The water turbines have been designed as small turbines with a diameter of 48 mm, and they are installed inside a 2-inch or 50.8-mm pipe. In this work, researchers designed a 2D model of domain C and a 3D model of a small water turbine wheel, deflector, and pipeline system by using Autodesk Flow Simulation. The control volume technique was used in the numerical simulation method, and the k-epsilon turbulence model was employed to find the computational results. When the appropriate element meshing for each model section was generated for numerical simulation in Computational Fluid Dynamics (CFD), it was found that the torque from the water turbine modelling changed based on the time domains and was connected to speed relative to the developed force. The next step is to collect the produced lift force, drag force, pressure coefficient (CP), torque, rotational speed, pressure drop, and output power for each turbine using computational fluid dynamics (CFD). Results obtained from Autodesk Flow Simulation have shown that a water flow of 0.0015 m³/s and a velocity of 0.74 m/s can run on the designed vertical-axis small water turbine, delivering 6.62 W of maximum mechanical power at 423.13 RPM. The higher the wind turbine efficiency is, more energy will be developed in Thailand.

1. Introduction

At present, water is essential for the livelihoods of the population of Thailand as it is required for consumption and business activities that include the automotive, food, and agricultural industries. All the things mentioned rely on water as an intermediary in their drives. In particular, agricultural activities in each region of Thailand that rely on water resources are the main factors for the implementation of activities in the form of dams, reservoirs, regional water supply, or in other ways other than those mentioned, etc. The transfer of water from the reservoir to the point of use relies on pipes of various sizes that work with high-pressure water pumps to drive the fluid. When considering Energy consumption, each fluid minute requires power, either in the form of electricity

* Corresponding author.

E-mail address: nat.kas@kmutt.ac.th (Nat Kasayapanand)

or fuel. With the global energy crisis, it is necessary to be more aware of energy [1]. Therefore, Developing and being able to generate energy sources from what is already available can be considered very useful at the present time. Water turbines installed inside pipes are also considered mechanical devices used as tools to extract energy generated by the movement of new flow patterns [2]. Hydroelectric power is considered a fully mature renewable energy source and is the most expensive source of renewable energy. It can be competitive and play an important role in today's mixed-use power generation strategy. It contributes to more than 16 percent of electricity generation worldwide and about 85 percent of the world's renewables [3].

Mosbahi *et al.*, [4] stated that electricity plays an important role in the development of the economy, directly or indirectly. Muhsen *et al.*, [5] found that the principle of energy extraction derived from water with various types of turbines in the pipeline or fluid pipeline system can be very useful at the present time as it will significantly reduce the cost of the system. According to Mosbahi *et al.*, [4] the Lucid Spherical is another form of water turbine that is continually being developed and installed into piping systems to convert fluid flow energy into electrical energy. According to past research reports, the installation of water turbine wheels in the pipe systems, which will be installed or connected to generators primarily from the top of the pipe [5-7]. Over the years, there has been a wide range of researchers and research around this field. Mabrouk *et al.*, have improved the efficiency of the water turbines that used to be installed in a large number of piping systems. The water turbine reel model used for setting up the pipe also has different features depending on the characteristics of the completed installation [6-8]. The most popular tools to design and improve the efficiency of water turbines in pipes are prefabricated fluid dynamics programs such as the ANSYS FLUENT program, Autodesk Simulation CFD, Autodesk Flow Simulation, and the COMSOL Multiphysics program. These program formats can perform calculations to solve systemic problems with continuity equations. Continuity equations and additionally allow to solve complex turbulence models [1,9].

For numerical simulation with computational fluid dynamics, the first thing to keep in mind is to prepare the right analytical model. Furthermore, taking into account the creation of different types of mesh elements to suit the analysis, such as the format of mesh elements, the number of node points, the number of layers of skin layers, etc., is essential. These variable values can be customized in the finished programs that make the selection. There are a lot of research studies around the effect of an appropriate number and type of mesh elements, which is the reason behind the importance of choosing the correct number and type of mesh elements for accurate and valid results. Devals *et al.*, [10] studied patterns of mesh element numbers that affect the accuracy and convergence of the answer to draft-tube turbine analysis. The Autodesk Flow Simulation software is another popular application for current fluid machinery design, due to the fact that it is already able to create a good mesh element and can perform a variety of analyses, including rotational analysis or fluid heat transfer, as well as free surface flow analysis [11]. The Autodesk Flow Simulation is a program that works well with SOLIDWORKS, Autodesk Inventor Professional, and Catia programs and supports 3D files used for analysis that come from many file extensions [12]. Under the principles mentioned above, the researchers were able to demonstrate a new type of energy generation. It relies on the flow of water inside the pipe that flows through the turbine wheels that are installed in the piping system. According to past research on water turbines installed within a piping system, it was found that the cost of design and production is very high due to the need to design pipe sizes with particular cross-sectional areas. It was also found that the installation still included some equipment inside the pipe, such as nuts and screws, which directly affected the loss of flow rate [2,3,13]. As a result of such installations and problems, the efficiency can be affected. And higher production costs will be required. The present water turbine generators for installation in pipelines have been studied,

investigated, and introduced through numerous research projects [14-19]. Therefore, the researchers wanted to propose a design for a wheel turbine generator and a small vertical turbine wheel unit for installation in a novel pipe. To solve the problem of installing water turbines in pipe systems that affect energy loss due to flow, reducing the cost of building special-sized pipes for the installation of water turbines and encouraging the use of items that are already on the market, such as PVC straight joints, can be some of the suggested solutions. Also, these solutions reduce the need for higher costs, as the design can be made usable and easy to maintain, and they are a guideline for developing new energy that can be installed on plumbing or agricultural pipelines in Thailand. This study aims to show the design of a new water turbine that reduces the installation process, can be attached to a PVC water pipeline available on the market without adapting the pipe size, and can reduce the effects of the flow loss rate caused by nuts and screws in the installation using computational fluid dynamics.

2. Methodology

2.1 Problem Formulation

According to past research on water turbines installed within a piping system, it was found that the cost of design and production is very high due to the need to design pipe sizes with particular cross-sectional areas. It was also identified that the installation includes some equipment inside the pipe, such as nuts and screws, which directly affect the loss of flow rate. When considering the fact that a water flow rate enters one end of a piping system and leaves the other, a pressure drop or pressure loss will occur due to the friction caused by fluids rubbing against piping components and the interior walls of a piping system, as shown in Figure 1.

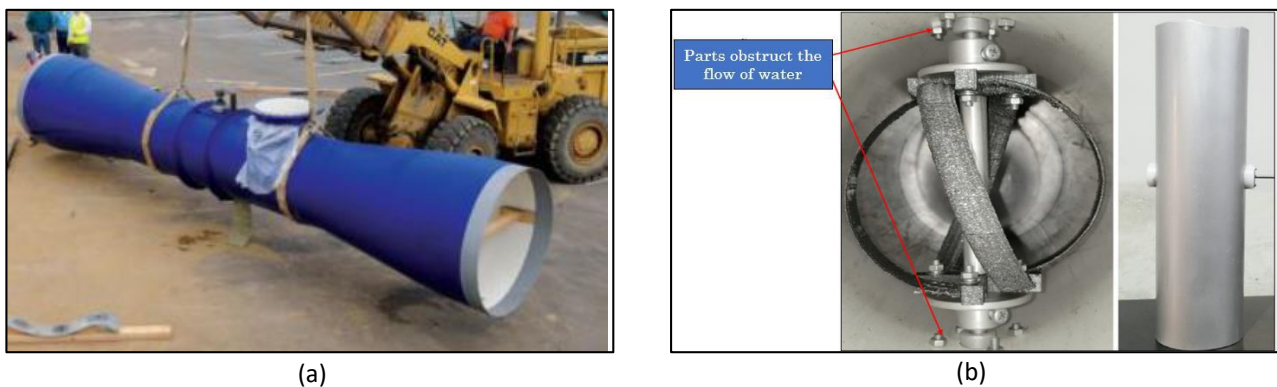


Fig. 1. The problems in this research are: (a) A specially designed water pipeline layout [3]; (b) Parts that obstruct the flow of water turbines in pipes [13]

2.2 Solution Methodology

2.2.1 CFD model

Predicting the flow of current flowing through the water turbine wheels that are installed in the piping system relies on the Navier-Stokes equation solving system. The Navier-Stokes equation consists of the equations of mass, momentum, and energy conservation rules. In addition, the research also applied a k-epsilon standard model ($k-\epsilon$) for calculating and simulating maximum rotation speeds [1,20]. The equations for the research can be written as follows:

$$\frac{\partial \rho}{\partial t} + \frac{\partial(\rho u_i)}{\partial x_i} = 0 \quad (1)$$

The k-epsilon turbulence model is one of the most widely used turbulence models in industry and research. The k term represents the turbulence kinetic energy, and ε is the turbulence eddy dissipation. Then, in Eq. (1), it was defined the equation of continuity, where ρ is the density of water, t is time, and represents the three spatial components of the fluid velocity u, v, w [14]. The momentum equations are defined by Eq. (2) and Eq. (3) in which k and ε are related, where are constant $C_{\varepsilon 1}, C_{\varepsilon 2}, \sigma_k, \sigma_\varepsilon$. The values of P_{kb} and represent the influence of buoyant forces [21-23, 25].

$$\frac{\partial(\rho k)}{\partial t} + \frac{\partial}{\partial x_j}(\rho U_j k) = \frac{\partial}{\partial x_j} \left[\left(\mu + \frac{\mu_t}{\sigma_k} \right) \frac{\partial k}{\partial x_j} \right] + P_k - \rho \varepsilon + P_{kb} \quad (2)$$

$$\frac{\partial(\rho \varepsilon)}{\partial t} + \frac{\partial}{\partial x_j}(\rho U_j \varepsilon) = \frac{\partial}{\partial x_j} \left[\left(\mu + \frac{\mu_t}{\sigma_\varepsilon} \right) \frac{\partial \varepsilon}{\partial x_j} \right] + \frac{\varepsilon}{k} (C_{\varepsilon 1} P_k - C_{\varepsilon 2} \rho \varepsilon + C_{\varepsilon 1} P_{\varepsilon b}) \quad (3)$$

The water turbine torque (T) is calculated by using Eq. (4), where S is the surface of the rotating parts, \vec{r} is the position vector, $\vec{\tau}$ is the total stress tensor, \hat{n} is a unit vector normal to the rotating surface, and \hat{a} is a unit vector parallel to the axis of rotation.

$$T = \left(\int_S \left[\vec{r} \times \left(\vec{\tau} \times \hat{n} \right) \right] ds \right) \times \hat{a} \quad (4)$$

2.2.2 Theory of rotation analysis

The free-spinning technique in the Autodesk Flow Simulation software used in the research has functions and patterns of control equations used for solving problems in calculating rotation in the relative frames of reference objects and fluids with free vortices [11], and the equation of rotational relationships can be written as follows:

$$a_t = \vec{r} \times \frac{\partial \vec{\Omega}}{\partial t} \quad (5)$$

Where a_t is the contact acceleration, \vec{r} is the wheel radius, $\vec{\Omega}$ is the angular speed, t is the time.

When considering the acceleration to the center of the rotating fluid. Equation relationships can be written as Eq. (6) [11].

$$a_{centrip} = \vec{\Omega} \times (\vec{r} \times \vec{\Omega}) \quad (6)$$

When $a_{centrip}$ is the acceleration to the center of rotation.

When considering this, it was found that acceleration is associated with the reference frame in which the rotation is performed. The observations of the Euler equation and centrifugal forces

depend on the position vector of the object, while the Coriolis force depends on the speed of the object measured in the rotating reference frame. A pattern for the correlation equation of the Coriolis acceleration can be written as in Eq. (7) [11].

$$a_{\text{coreolis}} = 2(\vec{W} \times \vec{\Omega}) \quad (7)$$

When a_{coreolis} is the Coriolis acceleration.

The speed in the inert frame is associated with the speed in the relative frame, with equations being able to write a pattern to show behaviour, as in Eq. (8) [11].

$$\vec{V} = \vec{W} \times \vec{\Omega} \times \vec{r} \quad (8)$$

When V is the speed in the inert frame for rotation.

For the range of time to analyze the rotation that surrounds the mesh for movement, the rate of change in the degree of rotation can be calculated from Eq. (9) [11].

$$\Delta\theta = 6\Delta t (RPM) \quad (9)$$

Where $\Delta\theta$ is the rates change of rotational, Δt is the rate of change in time intervals.

From Eq. (9), it can be seen that the rotational speed value is in rpm. The mesh part for moving and repositioning rotations is determined by the total scale volume, and it is paired from the rotated side to the non-rotating side of the sliding mesh element interface using geometric estimations between mesh systems. Both elements are then transferred on a predictive basis. In other words, when checking each flux page on the rotor and stator interfaces, flow patterns flowing from the rotor rotation to the stator increase the volume in the direction of flow. Similarly, the flow from stator to rotor shows data from the stationary mesh element to the rotating mesh element. In the case of the connection of the equation, momentum is transferred through the mesh zone. It can be shown that the rotation elements can be similar. When the speed of the rotation is unknown, angular momentum conservation is used to predict angular velocity versus the analysis period.

2.3 Time Step in Simulation

Computational fluid dynamics is related to the rotation of energy machinery, such as water turbines, wind turbines, or different types of water pumps. Most analytical models are transiently analyzed. What is needed is a proper step time, where the calculation equation for the time step [11] can be calculated from Eq. (10) [11].

$$T = D / (N \times 6) \quad (10)$$

Where T is the step time, D is the diameter of the wheel (m) and N is the rotation speed (RPM).

3. Methodology

The research was carried out in the Laboratory of Energy Technology, School of Energy, Environment, and Materials, at King Mongkut's University of Technology Thonburi in Thailand. In this study, a ratchet mounting kit consisting of a small generator, a set of frames 1 and 2, as well as a set of small vertical turbine wheels for installation in a novel pipe were designed for use in studies and

to be installed on the PVC pipes used in office buildings, houses, or fruit sections. When designing this experiment, the installation distance (300, 600, or 900 mm) between the turbines will be evaluated. Figure 2 depicts an overview of the experiments conducted in this study. The research process divides the content into three parts:

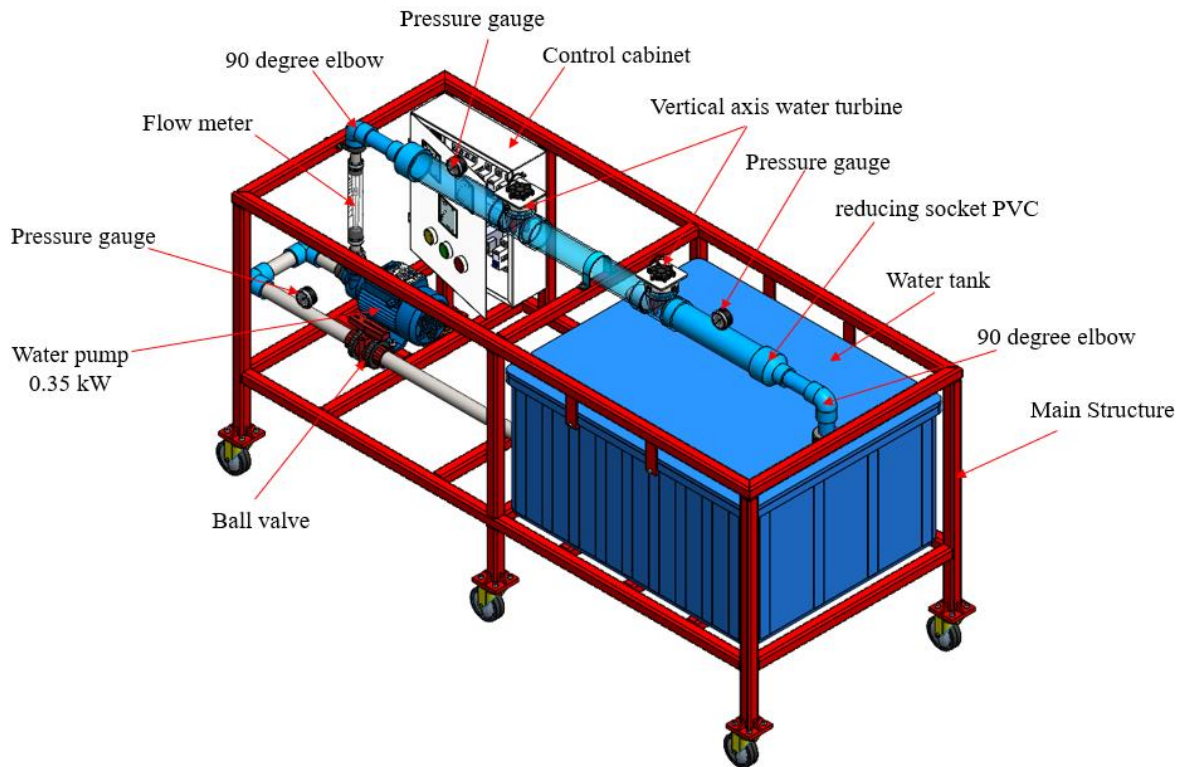


Fig. 2. Experimental setup of the vertical-axis small water turbine generator for installation in pipeline

3.1 Study the Angle of Laying Water Turbine Blades

In this section, a C-domain will be created to serve as a 2D model to analyze the different propeller shapes shown in Figure 3 in order to study and analyze angles that can generate good lifting forces and have minimal flow resistance. Air foil shapes such as 63-212, 4415, and Clark Y models were compared with the shape of the KMUTT blades created, while simulating and comparing them to calculate the variables of the L/D ratio throughout and calculating the pressure coefficient around the designed turbine blades, etc. From Figure 4 the computational domain has a width of 1,000 mm and a length of 1,500 mm and it was determined that the speed at the entrance to the C-domain is a component type with a constant speed of 0.74 m/s, and the exit area has a constant pressure of 0 pascal. The C-domain model was used to divide the shape and to determine the properties of the bias type at the boundaries of the shape division, as shown in Figure 4(b), and later used to create the mesh element for the C-domain model in this research, as shown in Figure 5, and the velocity results of the flow field within C-domain model can be displayed as shown in Figure 6.

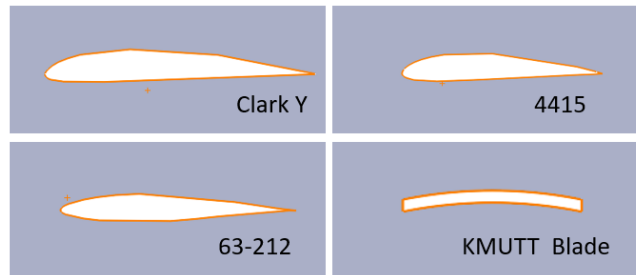


Fig. 3. The models of water blade shape different for analysis

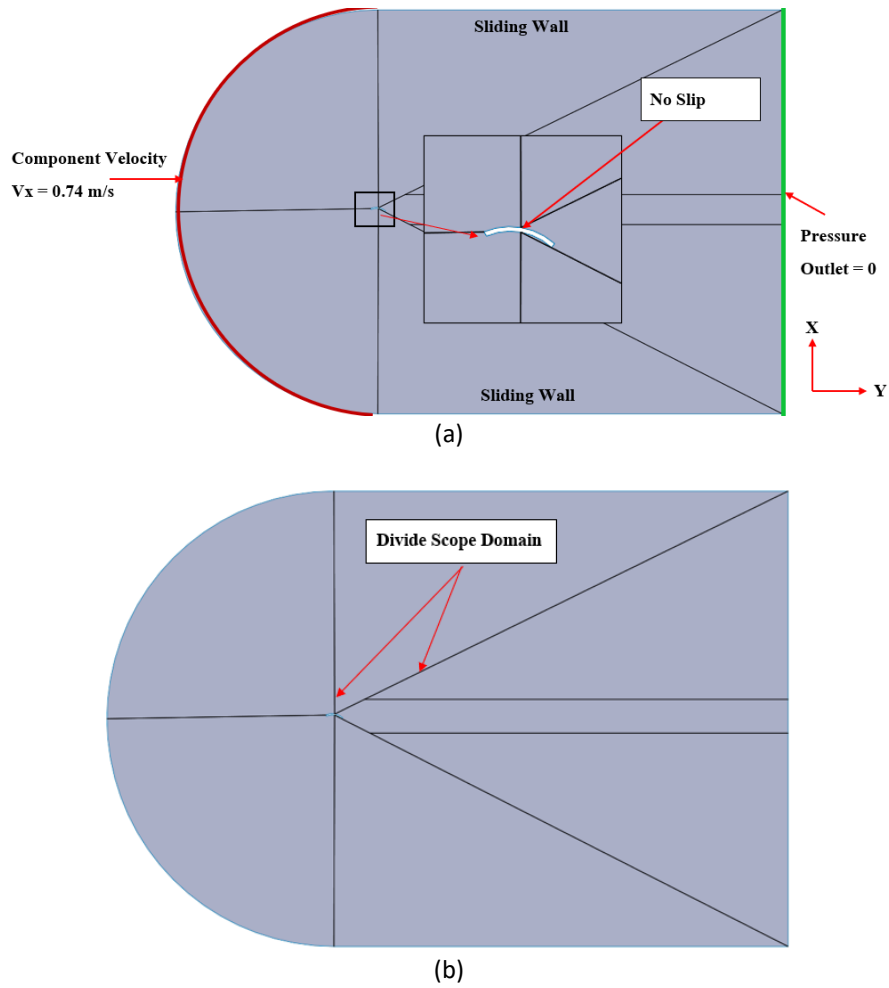


Fig. 4. The 2D model for (a) Boundary conditions and (b) Domain C in this research

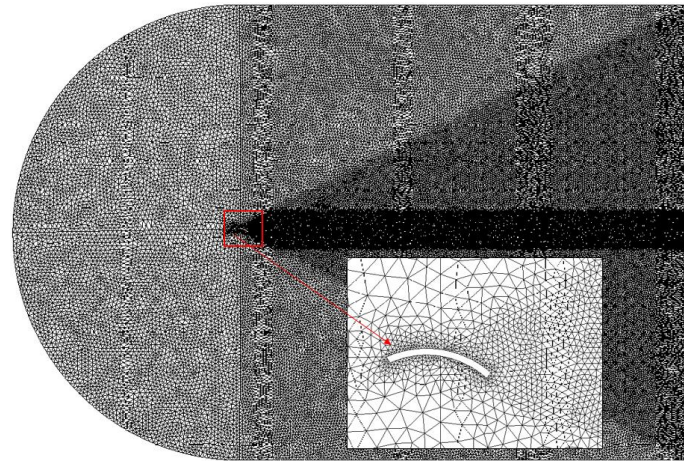


Fig. 5. The mesh element for domain C

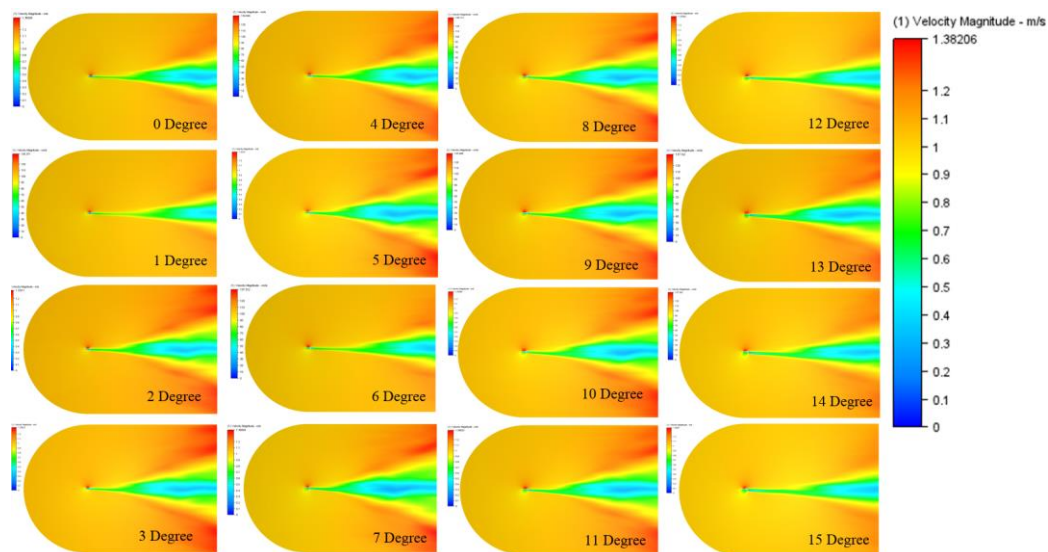


Fig. 6. The velocity results of the flow field within the C- domain

It visually depicts the appropriate amounts of meshing for the CFD water turbine model for various blade velocities, as determined by testing the water speed model at an inlet water speed of 0.74 m/s in Figure 5. The model shows the relationship between the number of mesh elements and the blade angle of the water turbine over a range of 10,000 to 500,000 elements. From Figure 6, the static pressure of the water is simply the weight per unit area under consideration. In this work, the amalgamation of static and dynamic pressure is known as total pressure. In the simulation, the angle from 0 to 15 degrees is determined which will be used for analysis to establish the lift force and drag force. In this section, angle starting at 0 degrees was considered. So, at an angle of attack of zero degrees, the contours of static pressure over an airfoil and KMUTT blade are symmetrical for the upper and lower sections, and the stagnation point is exactly at the nose of the airfoil and the KMUTT blade. Hence, there is no pressure difference created between the two faces of the airfoil and the KMUTT blade at zero degrees of attack. The numerical simulations used to calculate the angle of the turbine blades with a C-domain model showed that the shape of the KMUTT Blade has a greater L/D ratio than other models, and the highest value is at an angle of 12 degrees, as shown in Figure 7.

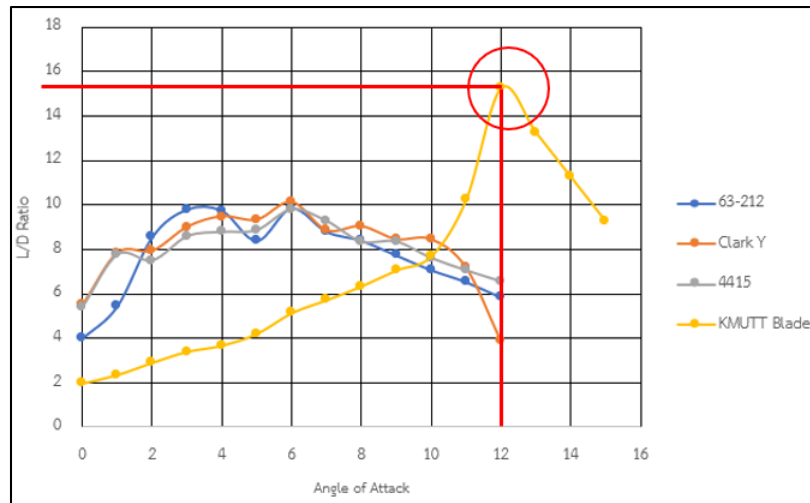


Fig. 7. The angle results from the simulation of the water attack on the turbine blade

The amalgamation of static and dynamic pressure is known as total pressure. According to the results of a simulation of the pressure coefficient around the shape of the airfoil and KMUTT blade shown in Figure 8, the Clark Y airfoil and the KMUTT blade have similar values.

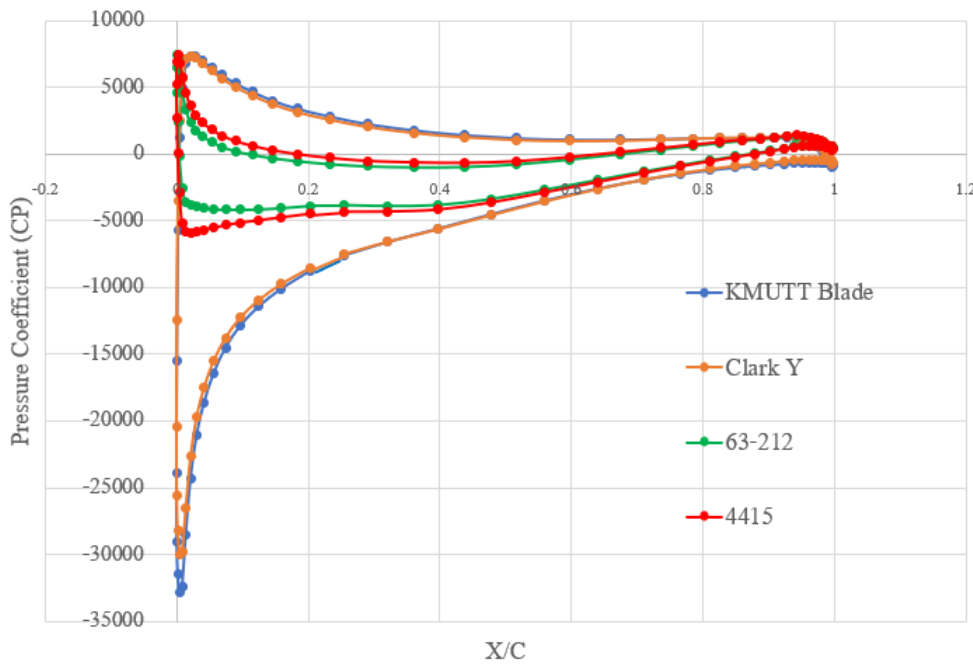


Fig. 8. Pressure coefficient results

3.2 3D Design for the Water Turbine Wheel

Using the variable correlations obtained from numerical simulations, it was found that KMUTT turbine blades at an angle of 12-degrees can provide good results in lifting and water flow resistance. Therefore, this angle was chosen in the design of the water wheel in this research. The researchers used variables of angles obtained from numerical simulations for designing small vertical-axis water turbine wheels and can show the result in Figure 9(a). Figure 9(b) shows the actual manufacturing of a small water wheel using 3D printing and plastic injection molding.

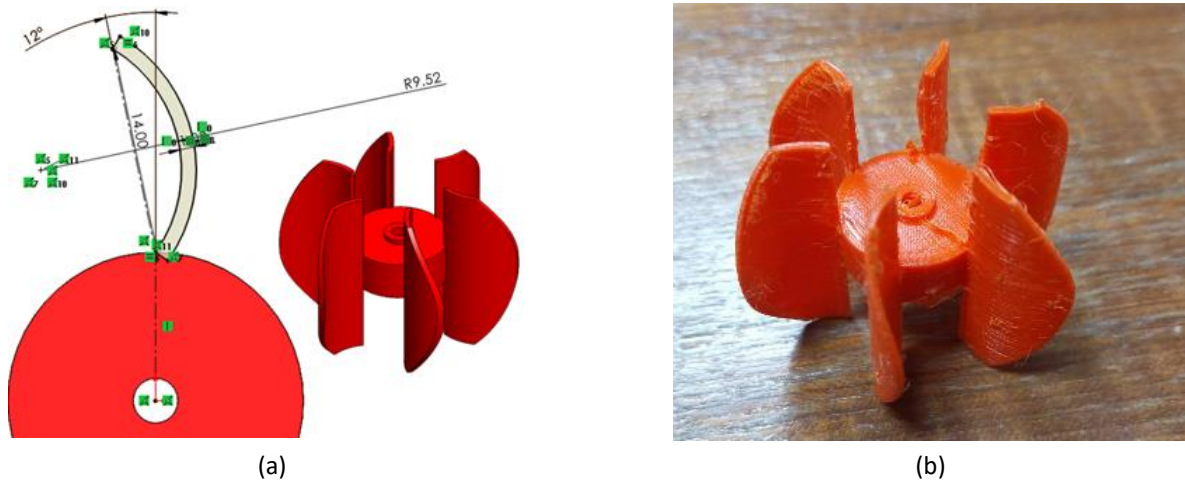


Fig. 9. Water turbine design results from (a) 3D design using computer software and (b) Actual production of a small water wheel using 3D printing

3.3 The Design of the Structure for the Water Turbine Wheel Installation

After designing the wheel of a small water turbine for installation in the water pipeline, the next step is to design a structure for installing a generator. In this part, using the principle of data consideration for the two-part design, the shape of the DC 12V Model GOSO F50-12V small generator, purchased from Shenzhen Global Technology, was determined. Then, the data will be considered, taking into account the installation location, so that it can be properly assembled into the pipeline and be easy to maintain. The design was intended to be installed in the joint range between two straight joints connected to the straight pipe, as shown in Figure 10. After considering the design data for both parts as mentioned above, the shape of frames one and two used for the installation of the water turbine wheels attached to the piping system can be seen in Figure 11.

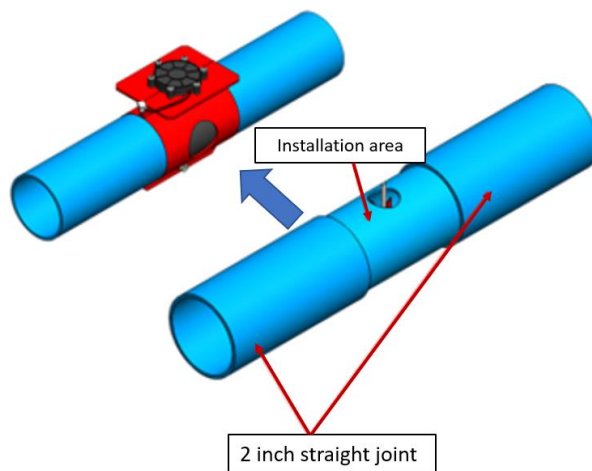


Fig. 10. The position of the splice ranges between two straight joints connected to the straight pipe

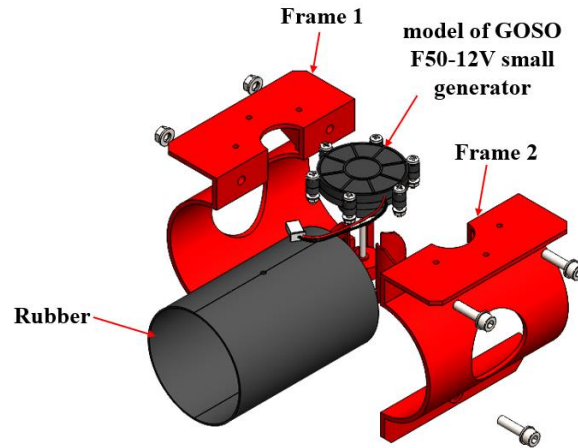


Fig. 11. The prototype of frame one and frame two parts used for the installation of generators and water turbine wheels

3.4 Procedures for CFD Simulation

In the Fluid Dynamics Analysis section, the installation distance between both wheels of water turbines will be evaluated from distances of 300, 600 and 900 mm. They are installed in pipes with a length of 1.1 m, as shown in Figure 12. From Figure 12, the pattern of water flow inside the pipe was studied while calculating the rotation speed in the free-spinning module in the Autodesk Flow Simulation program, as well as calculating the torque and power of the two turbines at different installation distances. In the initial condition determination procedure, the researchers determined the flow rate at the entrance to be 90 LPM, or $0.0015 \text{ m}^3/\text{s}$ or 0.74 m/s , set a constant pressure of 0 Pa at the exit and determined the inertia of the water turbine wheels to be equal to $0.00002304 \text{ kg}\cdot\text{m}^2$ choosing the turbulence model as k-epsilon.

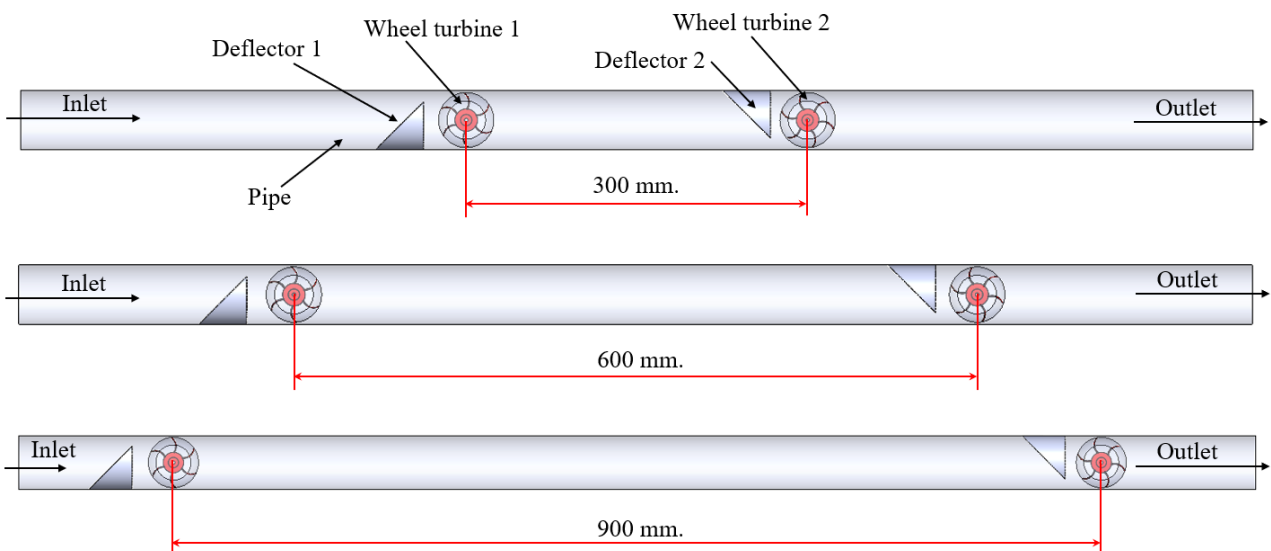


Fig. 12. The installation distance of both wheels of the water turbines at 300, 600, and 900 mm

The deflectors installed inside the water pipes in this research are at an angle of 30 degrees, as shown in Figure 12. The deflectors adjust to the direction of turbine rotation so that it can have a positive torque effect on the direction of turbine rotation.

4. Results

4.1 Free Spinning Analysis

In this section, when analyzing the results to calculate the free-spinning rotation speed, the variables related to the inertia moment value of the water turbine wheel, obtained from the design in Figure 9, were estimated. The test procedure will study the turbine wheels that are installed in conjunction with the pipeline system at different distances, as shown in Figure 12. The data from the 3D program can be obtained with the weight of the water turbine wheels used to calculate the inertia moment. In this study, the material used to build the water turbine wheels was the SAE 304 stainless steel and the weight of the wheels was estimated using the 2014 version of the Autodesk Inventor Professional program. The results showed that the designed wheels weighed 0.04 kg and the diameter of the water turbine wheels was 48 mm. After that, the measured weight was used to calculate the mechanical inertia moment. It can be calculated from Eq. (11) as follows:

$$I = mr^2 \quad (11)$$

Where I is the mechanical inertia moment (kg.m^2), m is the mass of the wheel (kg), r is the radius of wheel (mm).

The next step is to simulate numerical results to calculate rotation speed with the free-spinning analysis module. Techniques were used to find the tetrahedral elements of resolution in areas where high speeds and pressure changes occur. After that, different numerical models were created with its corresponding meshes with distinct element size values in the rotating domain zone: would organize this with bullets instead of adding it to text. The mesh element format as CFD was defined and the size of the mesh element in the section of the rotating domain zone was 1mm. The mesh size around the water turbine wheel is equal to 1 mm, in the deflector zone is 2 mm, in the pipeline zone is 3 mm, and the wall layer of the pipe was defined with 10 layers, with the value in the layer gradation section equal to 1.5, as shown in Figure 13. Similarly, in the section of the rotating domain zone, it is defined as a tetrahedral-type mesh element. In the rotating domain zone of the water turbine wheels, the first grid on the surface of the water turbine blade is made into a layer using the y^+ value setting of 10, and the layer gradation equals 1.5 as shown in Figure 14. The y^+ is defined as a non-dimensional distance [24]. The model shows the relationship between the number of elements and the rotational speed of the water turbine for installation in a water pipeline over a range of 100,000 to 600,000 elements. Thus, 600,000 elements were used in the CFD simulation.

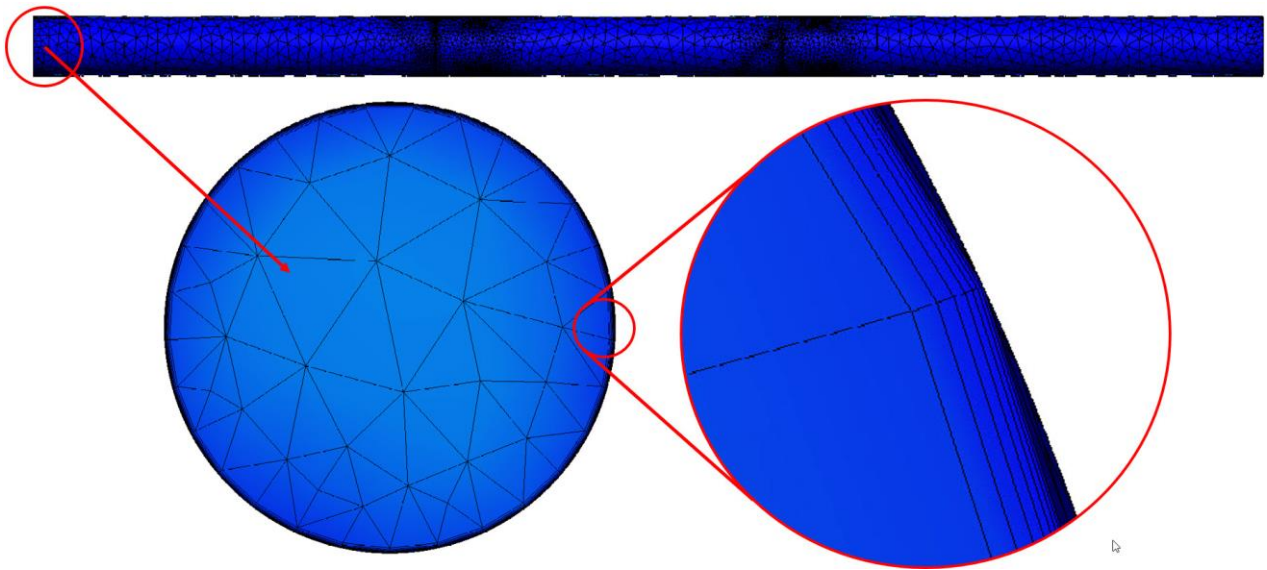


Fig. 13. The results of the pipeline's mesh elements

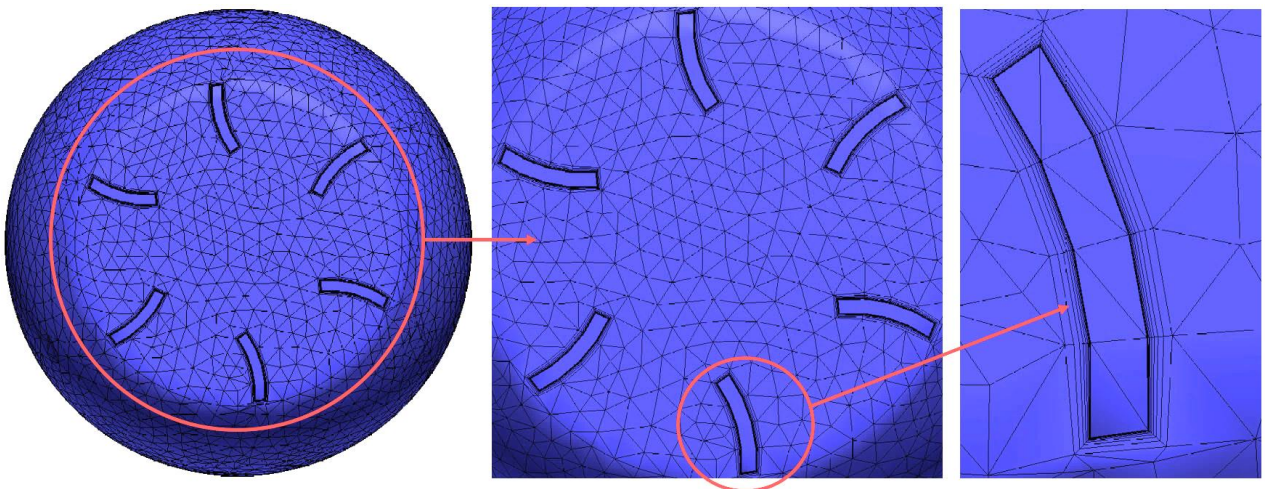


Fig. 14. The results of the mesh element creation for wheels and rotation zone

After that, in the free-spinning module, with a step time definition of 0.01, and setting the number of iterations for 1000, the result of plotting the contour speed within the water pipe flow field of analysis for free spinning rotation speed is shown in Figure 15 and the result of the rotation speed is shown in Figure 16 and Table 1.

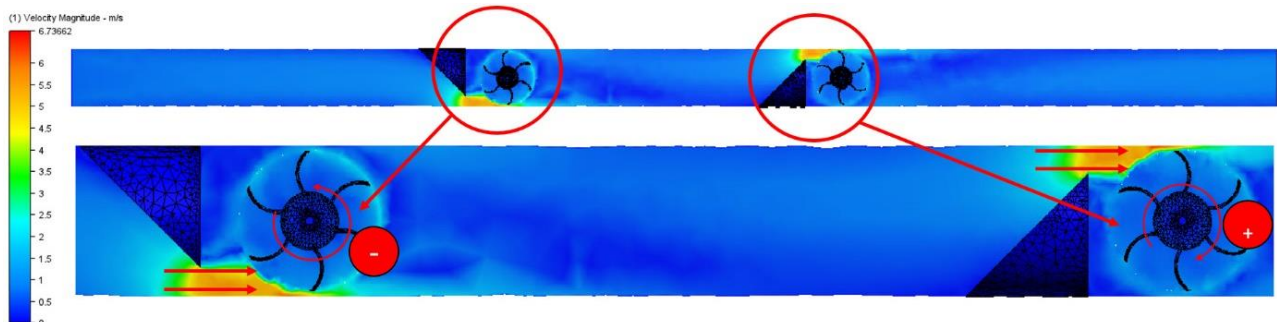


Fig. 15. The velocity results of the plot contour inside the water pipe flow field of analysis for free spinning

	Time (sec)	Hydraulic Torque (N-m)	Rotating Speed (RPM)		Time (sec)	Hydraulic Torque (N-m)	Rotating Speed (RPM)
988	9.88	0.000953707	-405.494	988	9.88	0.000841068	446.093
989	9.89	-0.000600029	-401.541	989	9.89	0.00065247	449.579
990	9.9	0.000308151	-404.028	990	9.9	0.000216125	452.283
991	9.91	-0.000475143	-402.751	991	9.91	-7.44324e-05	453.179
992	9.92	-0.000723578	-404.72	992	9.92	-0.000950144	452.87
993	9.93	0.000842277	-407.719	993	9.93	-0.00112359	448.932
994	9.94	-3.66934e-05	-404.228	994	9.94	-0.0010011	444.276
995	9.95	-2.70933e-05	-404.38	995	9.95	-0.00030941	440.126
996	9.96	-0.000694788	-404.493	996	9.96	-0.000687351	438.844
997	9.97	-5.05268e-05	-407.372	997	9.97	6.6246e-05	435.995
998	9.98	0.000491056	-407.582	998	9.98	-0.000297671	436.27
999	9.99	-0.000773029	-405.546	999	9.99	-7.32025e-05	435.036
1000	10	0.000534293	-408.75	1000	10	0.000201426	434.733

Fig. 16. The results of calculations for rotation speed with the free-spinning module

Table 1

The calculation results for rotational speeds at different installation distances

Installation distance	Wheel 1	Wheel 2	Average rotation speed of both wheels
300 mm	-408.75 RPM	434.74 RPM	421.75 RPM
600 mm	-412.12 RPM	430.24 RPM	421.18 RPM
900 mm	-416.42 RPM	429.84 RPM	423.13 RPM

4.2 Torque Analysis

For the torque analysis, computational fluid dynamics was used to help with the calculation and the determined residual value of all variables is less than 0.0001. If the calculation meets these criteria, the numerical calculation is considered to have approached the answer according to the preconditions. The study process begins by defining a rotating mesh element as a Moving Reference Frame (MRF) and defining the part that does not move as a stationary-type mesh element. This method is usually referred to as the Multiple Reference Frame (MRF). Based on the MRF technique, the results can be generated from the flow field by calculating torque, as shown in Figure 17 to Figure 19. According to Figure 17 to Figure 19, the results show that the vertical-axis small water turbine can generate energy as shown in Table 2.

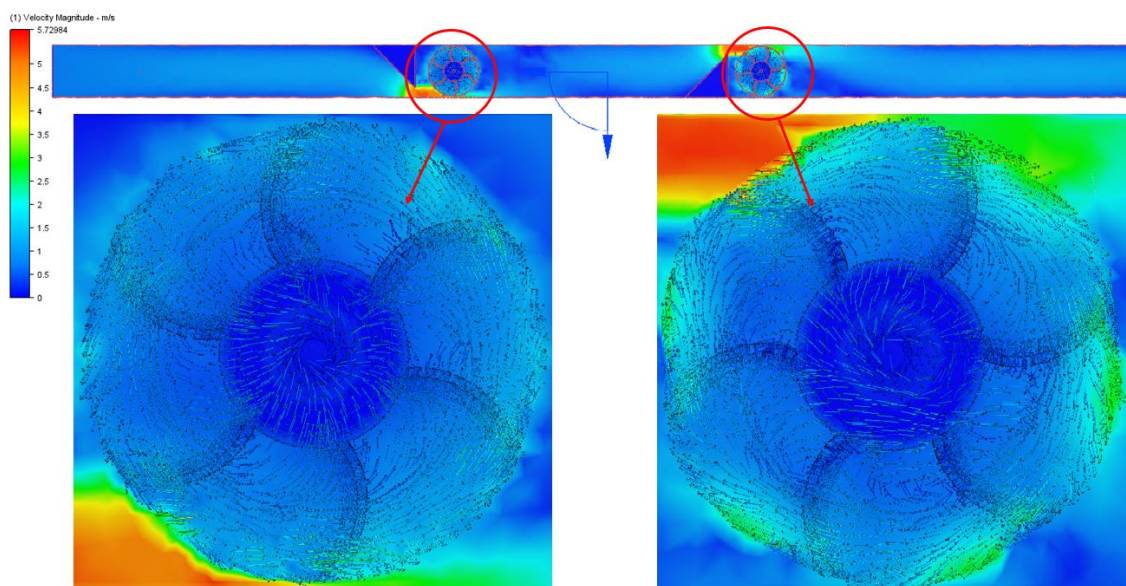


Fig. 17. The torque results on installation distance of 300 mm.

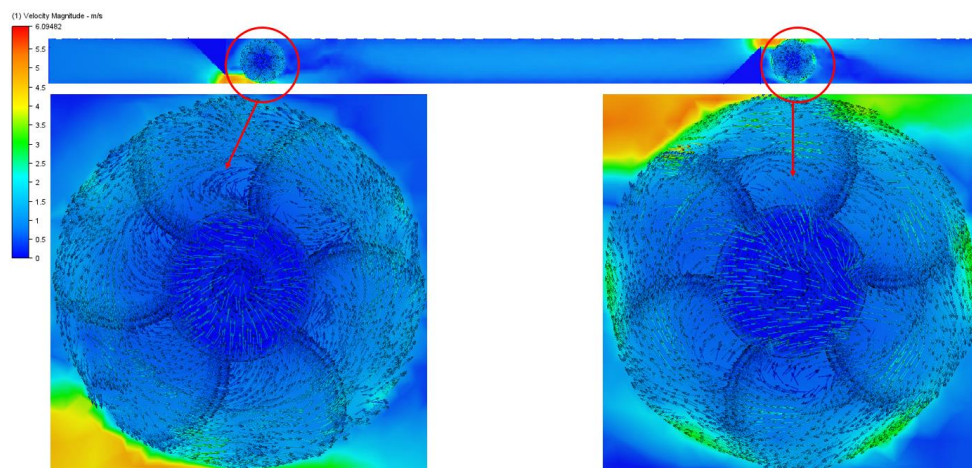


Fig. 18. The torque results on installation distance of 600 mm.

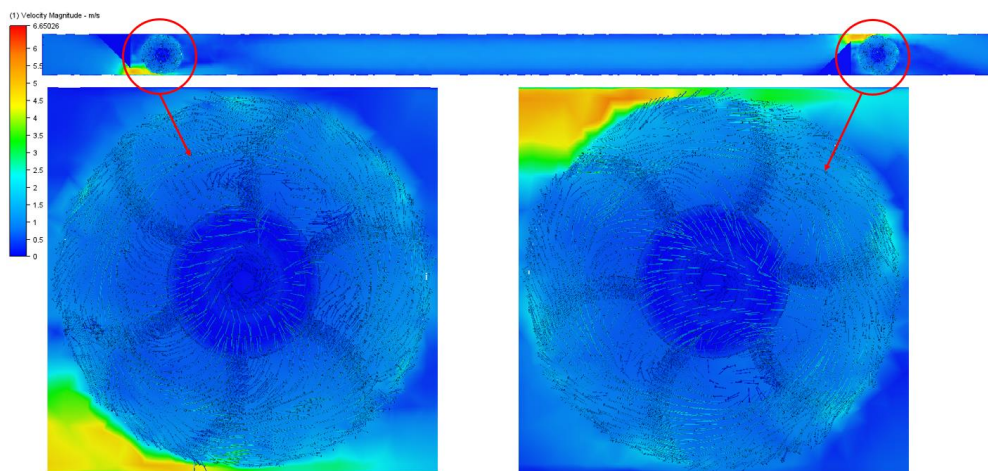


Fig. 19. The torque results on installation distance of 900 mm.

From Table 2, the torque generated by the computational fluid dynamics technique of a small turbine wheelset with a diameter of 48 mm installed in 2-inch water pipes at various installation distances was found to have similar results to Muhsen *et al.*, [5]. He studied and designed a turbine to be installed in a five-rotor H-Egg pipeline with a diameter of 49.5 mm. The results of the average torque are 0.046 N.m at a rotational speed of 333 rpm.

Table 2
 The results of torque and total power at various water turbine wheels distances

Water turbine wheel installation distance	Wheel 1	Wheel 2	Average torque	Total power output
300 mm.	0.069 N.m	0.073 N.m	0.142 N.m	6.28 W
600 mm.	0.077 N.m	0.070 N.m	0.147 N.m	6.49 W
900 mm.	0.080 N.m	0.070 N.m	0.150 N.m	6.62 W

4.3 Pressure Analysis

The vertical-axis small water turbine design is installed in the piping system. In this section, a deflector was installed into the piping system as shown in Figure 12. The deflector can increase the water speed entering the wheel of the water turbine to create a higher rotation speed. The installation of a deflector reduces the pressure drop at the exit destination. The static pressures from the CFD are shown in Figure 20, illustrating that static pressure occurred when the water flow made impact with the rotor blade. On the front and back sides of the rotor blade, higher pressures were found to be dependent on the higher water flows via an increase in the inlet water speed, as shown in Figure 20 and Figure 21.

Figure 21 shows a graph comparing the results of the pressure drop and the flow rate inside the pipeline for the installation of a novel vertical-axis small water turbine for the experimental model and CFD model for a water speed of 0.74 m/s. Water turbine generator installation distances of 300, 600, and 900 mm were found to produce similar pressure drop results. The CFD analysis of both wheels of the vertical-axis small water turbine for installation in the pipeline was carried out using Autodesk Flow Simulation software. In this study, the results from all the three different cases above can be summarized as following: With the analysis of the optimum angle for placing water turbine blades, it was discovered that the shape with the arc, as well as the KMUTT Blade, which was redesigned and compared to different airfoil shapes, as shown in Figure 8, and is commonly used to create turbine blades today [14], will result in a good lifting force. The results showed that the KMUTT blade was able to produce the best L/D ratio at an angle of 12 degrees, making the 12-degree angle a good choice to create the water turbine wheel and achieve the results shown in Figure 7.

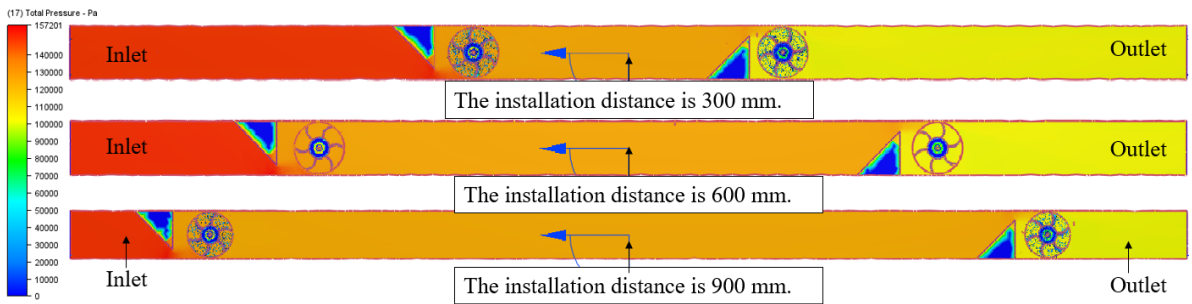


Fig. 20. The plot contour results for comparison of the total calculated pressure in the flow field

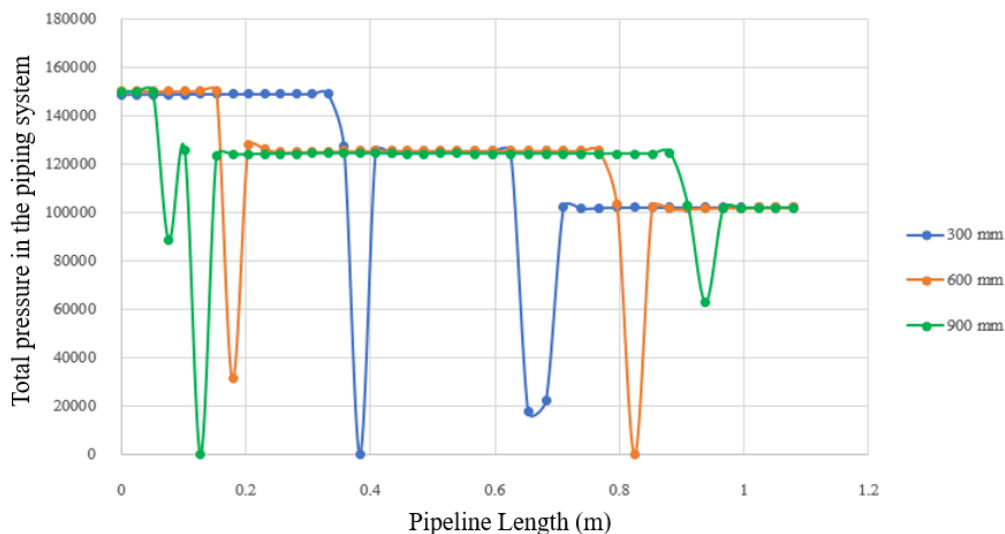


Fig. 21. The comparison of total pressure results of the flow field in the pipe system at different installation distances

The next step is the process of calculating the flow field to calculate rotation speeds with the free spinning module, where the turbine wheel model installation was divided into three range types: the installation distances of 300, 600, and 900 mm. The results of the tests showed that with the turbine installation distance of 300 mm, 600 mm and 900mm the rotational speeds that can be generated are between 408.75 and 434.74 RPM, 412.12 and 430.24 RPM and 416.42, 429.84 RPM, respectively. The negative rotation cycle indicates that the water turbine reels rotate counterclockwise. After that, the calculated rotation speed for the numerical analysis of torque and power output was calculated.

The results are presented in Table 2. From Table 2, the total electrical power model calculated from the different turbine installation distances showed that the installation range with a distance of 900 mm would generate a maximum of 6.62 W of power output, because the distance of the water turbine installation, at 900 mm, is adjacent to the water supply source more than any other installation position in comparison. The researchers calculated the total pressure in the pipe system equipped with the water turbine and deflector model. The installation of a deflector model into the piping system has the benefit of generating high water speeds before the run into the turbine blades, and the deflector modeling will directly affect the reduced pressure at the exit destination. Therefore, the appropriate shape should be designed and studied as part of the deflector model to further reduce pressure loss in the piping system.

5. Conclusions

The results of the new design of the vertical-axis small water turbine are generated for installation in pipes. It was found that the optimal propeller placement angle was 12 degrees, opting for the KMUTT Blade, and the wheels obtained from the design were able to generate an average maximum rotation cycle of 423.13 RPM at a distance of installation of 900 mm. A vertical-axis small water turbine generated for installation in pipes can generate a maximum of 6.62 W of power output. In future research, this multiple reference frame (MRF) technique could be applied to water turbines for installation in the pipeline. The free spinning module in Autodesk Flow Simulation can be used to investigate the effects of the water attack angle on the turbine blade and can be evaluated for different performances.

Acknowledgement

The researcher would like to thank all who assisted in this study, including the team at the Division of Energy Technology, School of Energy, Environment, and Materials, King Mongkut's University of Technology Thonburi, who supported the work and helped obtain a high-quality and accurate analysis. Furthermore, the authors would like to thank all of their friends who provided encouragement and support. The first author would also like to thank his family for their spiritual encouragement throughout the process of writing this paper.

References

- [1] Oladosu, Temidayo Lekan, and Olufemi Adebola Koya. "Numerical analysis of lift-based in-pipe turbine for predicting hydropower harnessing potential in selected water distribution networks for waterlines optimization." *Engineering Science and Technology, an International Journal* 21, no. 4 (2018): 672-678. <https://doi.org/10.1016/j.jestch.2018.05.016>
- [2] Payambarpour, S. Abdolkarim, Amir F. Najafi, and Franco Magagnato. "Investigation of blade number effect on hydraulic performance of in-pipe hydro savonius turbine." *International Journal of Rotating Machinery* 2019 (2019). <https://doi.org/10.1155/2019/8394191>
- [3] Casini, Marco. "Harvesting energy from in-pipe hydro systems at urban and building scale." *International Journal of Smart Grid and Clean Energy* 4, no. 4 (2015): 316-327. <https://doi.org/10.12720/sgce.4.4.316-327>
- [4] Mosbahi, Mabrouk, Ahmed Ayadi, Ibrahim Mabrouki, Zied Driss, Tullio Tucciarelli, and Mohamed Salah Abid. "Effect of the converging pipe on the performance of a lucid spherical rotor." *Arabian Journal for Science and Engineering* 44 (2019): 1583-1600. <https://doi.org/10.1007/s13369-018-3625-0>
- [5] Muhsen, Hani, Mariam Ibrahim, Ahmad Alsheikh, Mohammed Qanadilo, and Abdallah Karadsheh. "Turbine design and its impact on energy harvesting from in-pipe hydro systems." *International Journal of Mechanical Engineering and Robotics Research* 8, no. 5 (2019): 685-690. <https://doi.org/10.18178/ijmerr.8.5.685-690>
- [6] MMSRS, Bhargav, Ratna Kishore V, and Anbuudayasankar SP. "Power generation by high head water in a building using micro hydro turbine—a greener approach." *Environmental Science and Pollution Research* 23 (2016): 9381-9390. <https://doi.org/10.1007/s11356-015-5317-6>
- [7] Muratoglu, Abdullah, and Muhammed Sungur Demir. "Modeling spherical turbines for in-pipe energy conversion." *Ocean Engineering* 246 (2022): 110497. <https://doi.org/10.1016/j.oceaneng.2021.110497>
- [8] Mutlu, Y., and M. Çakan. "Evaluation of in-pipe turbine performance for turbo solenoid valve system." *Engineering Applications of Computational Fluid Mechanics* 12, no. 1 (2018): 625-634. <https://doi.org/10.1080/19942060.2018.1506364>
- [9] Bianchini, Alessandro, Francesco Balduzzi, Peter Bachant, Giovanni Ferrara, and Lorenzo Ferrari. "Effectiveness of two-dimensional CFD simulations for Darrieus VAWTs: a combined numerical and experimental assessment." *Energy Conversion and Management* 136 (2017): 318-328. <https://doi.org/10.1016/j.enconman.2017.01.026>
- [10] Devals, C., T. C. Vu, Y. Zhang, J. Dompierre, and F. Guibault. "Mesh convergence study for hydraulic turbine draft-tube." In *IOP Conference Series: Earth and Environmental Science*, vol. 49, no. 8, p. 082021. IOP Publishing, 2016. <https://doi.org/10.1088/1755-1315/49/8/082021>
- [11] Autodesk Simulation CFD, Autodesk Simulation CFD, Produced by Autodesk Inc., 2021, <http://www.autodesk.com/cfd>. Accessed on 12 September 2022.
- [12] Autodesk Inventor, Autodesk Inventor Professional, Produced by Autodesk Inc., 2015, <http://www.autodesk.com/inventor>. Accessed on 18 August 2022.
- [13] Aziz, Muhammad Shahbaz, Muhammad Adil Khan, Harun Jamil, Faisal Jamil, Alexander Chursin, and Do-Hyeun Kim. "Design and analysis of in-pipe hydro-turbine for an optimized nearly zero energy building." *Sensors* 21, no. 23 (2021): 8154. <https://doi.org/10.3390/s21238154>
- [14] Hu, Zhuohuan, Dongcheng Wang, Wei Lu, Jian Chen, and Yuwen Zhang. "Performance of vertical axis water turbine with eye-shaped baffle for pico hydropower." *Frontiers in Energy* (2020): 1-14. <https://doi.org/10.1007/s11708-020-0689-9>
- [15] Diab, Ghada, Mohamed Elhakeem, and Ahmed MA Sattar. "Performance assessment of lift-based turbine for small-scale power generation in water pipelines using OpenFOAM." *Engineering Applications of Computational Fluid Mechanics* 16, no. 1 (2022): 536-550. <https://doi.org/10.1080/19942060.2021.2019129>

- [16] Chen, Huixiang, Kan Kan, Haolan Wang, Maxime Binama, Yuan Zheng, and Hui Xu. "Development and numerical performance analysis of a micro turbine in a tap-water pipeline." *Sustainability* 13, no. 19 (2021): 10755. <https://doi.org/10.3390/su131910755>
- [17] Hasanzadeh, N., S. Abdolkarim Payambarpour, Amir F. Najafi, and Franco Magagnato. "Investigation of in-pipe drag-based turbine for distributed hydropower harvesting: Modeling and optimization." *Journal of Cleaner Production* 298 (2021): 126710. <https://doi.org/10.1016/j.jclepro.2021.126710>
- [18] Jiyun, Du, Yang Hongxing, Shen Zhicheng, and Guo Xiaodong. "Development of an inline vertical cross-flow turbine for hydropower harvesting in urban water supply pipes." *Renewable Energy* 127 (2018): 386-397. <https://doi.org/10.1016/j.renene.2018.04.070>
- [19] Ma, Tao, Hongxing Yang, Xiaodong Guo, Chengzhi Lou, Zhicheng Shen, Jian Chen, and Jiyun Du. "Development of inline hydroelectric generation system from municipal water pipelines." *Energy* 144 (2018): 535-548. <https://doi.org/10.1016/j.energy.2017.11.113>
- [20] Cifuentes, Oscar Darío Monsalve, Jonathan Graciano Uribe, and Diego Andrés Hincapié Zuluaga. "Numerical Simulation of a Propeller-Type Turbine for In-Pipe Installation." *Journal of Advanced Research in Fluid Mechanics and Thermal Sciences* 83, no. 1 (2021): 1-16. <https://doi.org/10.37934/arfmts.83.1.116>
- [21] Lahamornchaiyakul, Werayoot. "The CFD-Based Simulation of a Horizontal Axis Micro Water Turbine." *Walailak Journal of Science and Technology (WJST)* 18, no. 7 (2021): 9238-16. <https://doi.org/10.48048/wjst.2021.9238>
- [22] Chen, Jian, H. X. Yang, C. P. Liu, C. H. Lau, and M. Lo. "A novel vertical axis water turbine for power generation from water pipelines." *Energy* 54 (2013): 184-193. <https://doi.org/10.1016/j.energy.2013.01.064>
- [23] Tahir, Muhammad Hamza, Shoukat Ali Mugheri, Salman Ahmad, Mughees Shahid, Nouman Zaffar, Muhammad Arsalan Malik, and Muhammad Asad Saeed. "Production of electricity employing sewerage lines using a micro cross flow turbine." *International Journal of Engineering, Science and Technology* 12, no. 2 (2020): 67-77. <https://doi.org/10.4314/ijest.v12i2.8>
- [24] Setiawan, Priyo Agus, Triyogi Yuwono, Wawan Aries Widodo, Eko Julianto, and Mardi Santoso. "Numerical study of a circular cylinder effect on the vertical axis Savonius water turbine performance at the side of the advancing blade with horizontal distance variations." *International Journal of Renewable Energy Research* 9, no. 2 (2019): 978-985.
- [25] Kunalan, Kerishmaa Theavy. "A Performance Investigation Of A Multi Staged Hydrokinetic Turbine For River Flow." (2021). <https://doi.org/10.37934/progee.17.1.1731>